THE JOURNAL OF PHYSICAL CHEMISTRY B

Article

pubs.acs.org/JPCB

Multinuclear NMR Study of the Effect of Acid Concentration on Ion Transport in Phosphoric Acid Doped Poly(benzimidazole) Membranes

Sophia Suarez,*[,†] N. K. A. C. Kodiweera,[‡] P. Stallworth,[‡] Seonghan Yu,[§] S. G. Greenbaum,[‡] and B. C. Benicewicz[§]

[†]Department of Physics, Brooklyn College/CUNY, Brooklyn, New York 11210, United States

[‡]Department of Physics and Astronomy, Hunter College/CUNY, New York, New York 10065, United States

[§]Department of Chemistry and Biochemistry, University of South Carolina, Columbia, South Carolina 29208, United States

ABSTRACT: ^{1}H and ^{31}P NMR spectra, line widths, spin−lattice relaxation times (T_1), and ^{1}H self-diffusion coefficients (D) were determined for two distinct poly(benzimidazole) (PBI) proton exchange membranes (PEM), para-PBI and dihydroxy-PBI (2OH-PBI), both incorporating varying concentrations of phosphoric acid. The study was performed over the temperature range of 20−180 °C, for phosphoric acid concentrations of 30, 50, and 70 wt %. Of the two samples, less mobility was indicated for the 2OH-PBI compared with the para-PBI at all acid concentrations. It was also observed that increasing the acid content resulted in an increase in the temperature at which the T_1 minimum or plateau occurred. ^{31}P spectra reveal the presence of pyrophosphates and in the case of the 50 and 70 wt % para-PBI samples higher oligomers such as tripolyphosphates. ^{1}H D data showed the 30 wt % para-PBI having almost identical values as the 70 wt % 2OH-PBI over the entire temperature range. In general, stronger short- and long-range interactions were observed in the 2OH-PBI matrix, yielding reduced translational proton transport compared to that of para-PBI. While these stronger interactions hinder translational proton diffusion, they could enhance proton transport by the Grotthuss or structure diffusion mechanism, the more favorable transport mechanism. Activation energies obtained from the ^{1}H D data supports a proton-hopping mechanism, with possible assistance from fast exchange between phosphate groups.

INTRODUCTION

High-temperature (100−200 °C) proton exchange membrane (PEM) fuel cells have been viewed as replacement power sources for automobile, residential, and commercial applications. High-temperature operation of PEM fuel cells affords a number of advantages. Among them are the following: greater carbon monoxide (CO) tolerance of the membrane electrode assemblies (MEA's), so that hydrogen produced by reforming hydrocarbons can be used without CO removal; reduction in water management; and greater efficiency in waste heat utilization. Their development, however, has been hindered by a number of factors, mainly the availability of high-temperature PEM's.

Membranes used in high-temperature fuel cells should not rely on the presence of water to facilitate efficient ion transport. Therefore, the use of traditional perfluorosulfonic acid membranes such as Nafion is severely limited. Several different classes of polymers have been considered for the development of high-temperature PEM fuel cells, including modified perfluorosulfonic acid, alternative sulfonated polymers, and acid−base polymer membranes.[1−3] The membranes are expected to have good thermal, chemical, and mechanical stability, in addition to high proton conductivity. In the acid−base polymer membrane category, poly(benzimidazole) (PBI), an amorphous basic linear polymer, is known to possess high thermal stability due to its high glass transition temperature (425−436 °C), and good chemical resistance.[4] In its natural state it is non-ion-conducting. However, when doped with acids, it demonstrates an Arrhenius type ionic conductivity that depends on the acid concentration, temperature, and humidity, thus making it an attractive candidate as a high-temperature fuel cell electrolyte.[5,6] In addition to this, PBI is more cost effective compared with fluorinated perfluorosulfonic acid polymers, and has low permeability to O_2, H_2, and CH_3OH.[7] Acids tested in PBI includes sulfuric (H_2SO_4), phosphoric (H_3PO_4), hydrochloric (HCl), perchloric ($HClO_4$), and nitric (HNO_3).[8] It was determined that high proton conductivity could only be obtained with amphoteric acids. Of the above-mentioned acids, the best dopant was thus found to be phosphoric.[9] In addition to this, phosphoric acid has high thermal stability and low vapor pressure at elevated temperatures.

The purpose of this study is to compare the transport properties of PBI incorporating varying phosphoric acid concentrations prepared by the polyphosphoric acid (PPA) process.[10,11] The two polymers chosen for this study were para-PBI, which has significant commercial relevance, and 2OH-PBI, which has exhibited one of the highest proton conductivities in membrane form as compared to many PBI derivatives examined to date. This method involves the use of PPA as both polycondensation reagent to produce high-molecular-weight polymers and casting solvent for film preparation in a one-pot procedure.[10,11] Previous data on phosphoric acid doped PBI membranes showed proton

Received: May 16, 2012
Revised: September 14, 2012
Published: September 18, 2012

ACS Publications © 2012 American Chemical Society

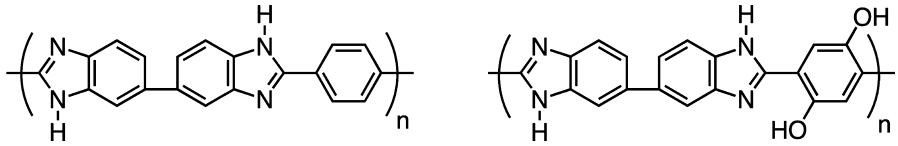

Figure 1. Chemical structures of PBI membranes used in this study: (left) para-PBI and (right) 2OH-PBI.

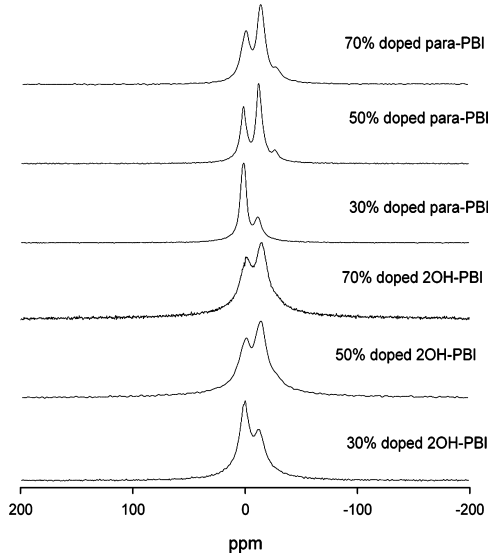

Figure 2. ^{31}P spectra for 2OH-PBI and para-PBI with 30, 50, and 70% phosphoric acid concentration at 50 °C.

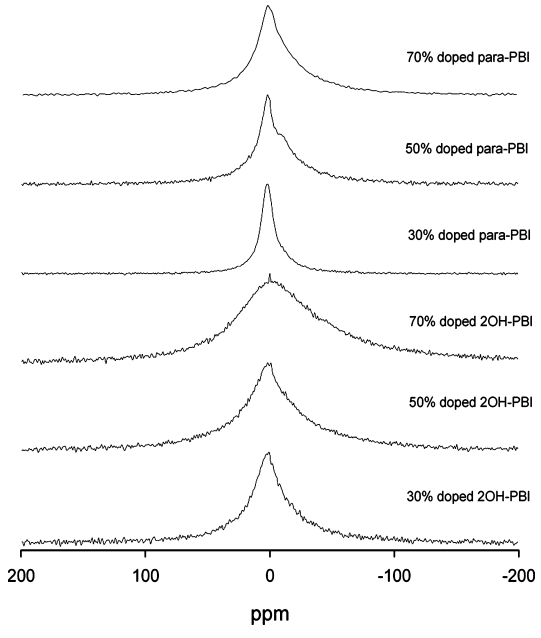

Figure 3. ^{31}P spectra for 2OH-PBI and para-PBI with 30, 50, and 70% phosphoric acid concentration at 150 °C.

transport by the Grotthuss mechanism, with assistance from the fast short-range exchange of the phosphate nuclei between the pyrophosphate and ortho phosphoric acid groups.[12] These membranes initially contained some water, and even with drying at elevated temperatures, it is possible that water molecules still remain in the matrix. In this study, the membranes are water-free, and the purpose is to characterize their transport processes. Toward this goal, nuclear magnetic resonance (NMR) measurements

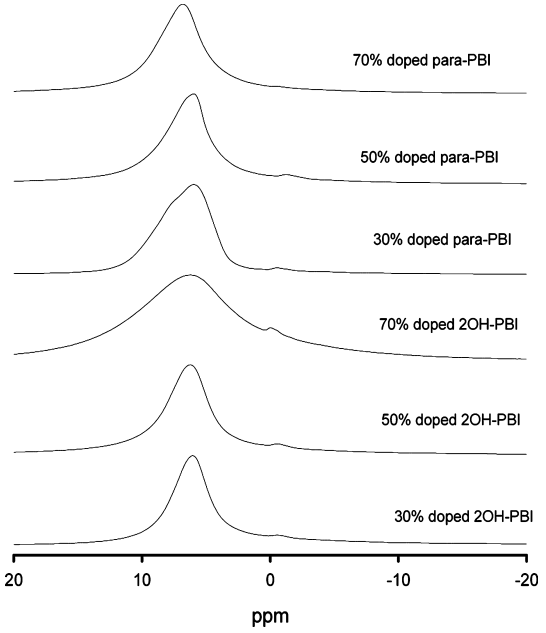

Figure 4. ^{1}H spectra for 2OH-PBI and para-PBI with 30, 50, and 70% phosphoric acid concentration at 50 °C.

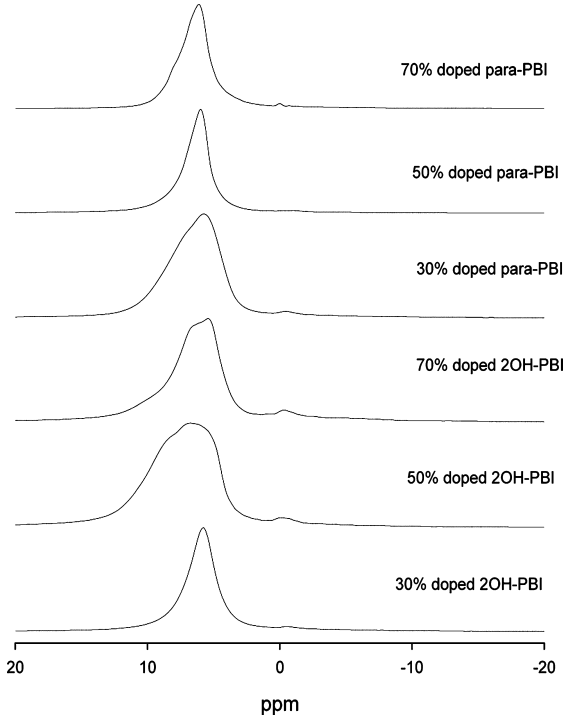

Figure 5. ^{1}H spectra for 2OH-PBI and para-PBI with 30, 50, and 70% phosphoric acid concentration at 150 °C.

such as spin−lattice relaxation times, self-diffusion coefficients, line widths, and spectra were performed for both polymers as a

dx.doi.org/10.1021/jp304761t | J. Phys. Chem. B 2012, 116, 12545−12551

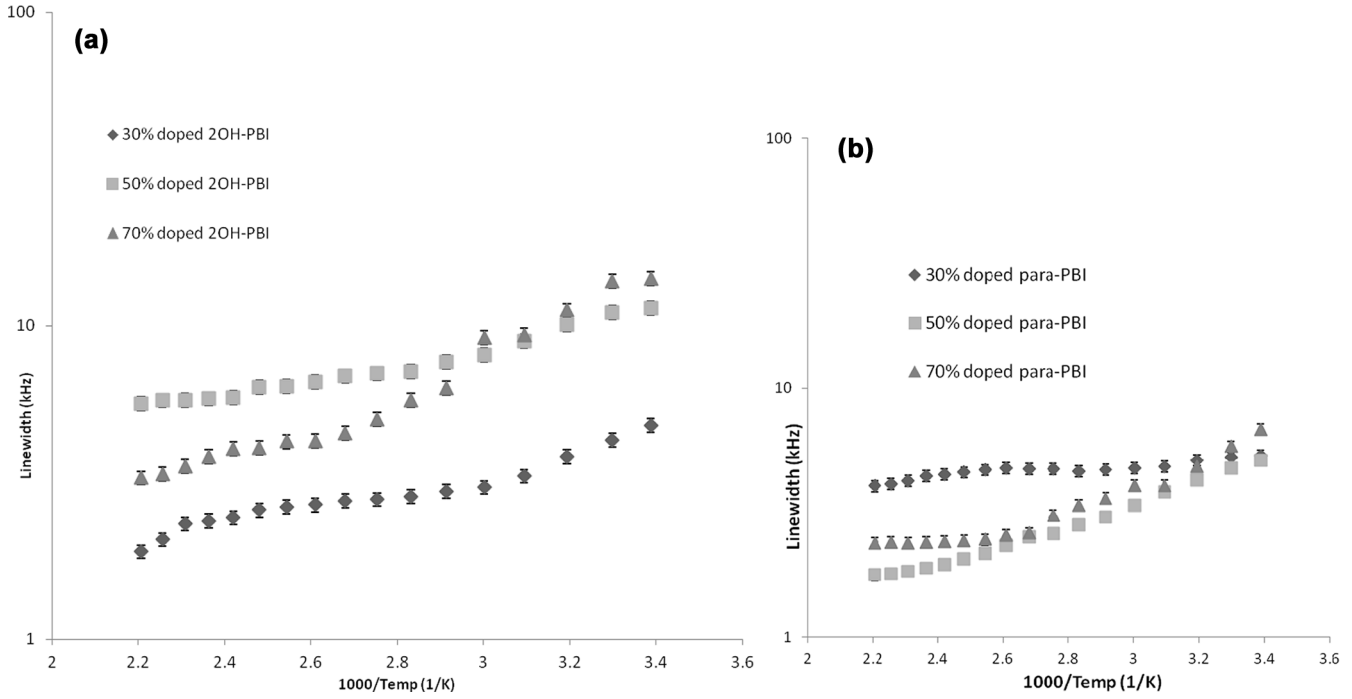

Figure 6. ^{1}H line-width data for (a) 2OH-PBI and (b) para-PBI with 30, 50, and 70% phosphoric acid concentration as function of temperature.

function of temperature and acid concentration, as they are able to provide information on the mass dynamics and structural environments on both a short (μs) and long (ms) time range.

EXPERIMENTAL SECTION

In this study, two PBI samples prepared by different methods were investigated. The samples were phosphoric acid doped para-PBI (Figure 1a) and dihydroxy-PBI (2OH-PBI) (Figure 1b), both methods have been previously described.[10] The phosphoric acid concentrations used were 30, 50, and 70%.

For NMR measurements, samples were dried at 150 °C in an oven for 2 h and packed into 5 mm o.d. × 20 mm NMR tubes and sealed. NMR measurements were performed on a Varian Direct Digital Drive spectrometer with ^{1}H Larmor frequencies of 301.02 MHz and a ^{31}P frequency of 121.85 MHz. Spectra, spin−lattice relaxation times (T_1), and self-diffusion coefficients (D) were obtained as a function of temperature. Spectroscopic references were water for ^{1}H and 85% H_3PO_4 for ^{31}P. Spectral information was obtained by Fourier transforming the resulting free-induction decay (FID) of single $\pi/2$ pulse sequence. Self-diffusion coefficients were obtained by the NMR pulse gradient spin−echo technique (NMR-PGSE), using the Hahn spin−echo pulse sequence ($\pi/2-\tau-\pi$).[13] For a diffusing system in the presence of a magnetic field, the application of square-shaped magnetic gradients of magnitude g and duration δ results in attenuation of the echo amplitude A. This attenuation may be represented by $A(g) = \exp[-\gamma^2 g^2 D\delta^2(\Delta - (\delta/3))]$, where γ, D, δ, and Δ represent the nuclear gyromagnetic constant, self-diffusion coefficient, gradient pulse width, and gradient delay, respectively. Applied gradient strengths (g) ranged from 1.5 to 900 G/cm. δ and Δ ranged from about 1.9 to 3.0 and from 4 to 5 ms, respectively. The resulting echo profile versus gradient strengths was fitted to the above equation and D was extracted. Spin−lattice relaxation times (T_1) were evaluated from inversion recovery ($\pi-\tau-\pi/2$)[14] measurements. T_1 was extracted by fitting the spectrum intensity represented by M vs τ, the pulse separation, for an array of τ values according to the equation $M = M_0 \cdot (1 - 2e^{-\tau/T_1})$ The temperature range studied was 20−180 °C with equilibration times of 15−20 min following each temperature change.

RESULTS AND DISCUSSION

1. ^{31}P and ^{1}H Spectra. ^{31}P spectra are shown in Figures 2 and 3 for two temperatures, −50 and 150 °C, respectively, for both the 2OH-PBI and para-PBI samples. At 50 °C, two components are clearly observed for the 30% para-PBI sample, while three components are observed or inferred in the 2OH-PBI, and 50 and 70 wt % para-PBI samples. The chemical shifts of the peaks are ∼0, −12, and −24 ppm, respectively, from left to right. The ∼0 ppm peak is assigned to free orthophosphoric acid as it corresponds to the reference 85% H_3PO_4 chemical shift. The ∼−12 ppm and −24 ppm peaks are assigned to the pyrophosphate and higher oligomers such as tripolyphosphate, respectively.[15]

At 150 °C a single asymmetric component with chemical shift ∼2 ppm is observed for the 2OH-PBI samples, the line width of which increases with increasing phosphoric acid (PA) content. This suggests that there is temperature-activated exchange between the phosphorus sites. While similar behavior was observed for the para-PBI samples, the line width at each acid content was smaller compared to the 2OH-PBI samples. This suggests the exchange between the various phosphorus sites in the para-PBI is faster. The differences in line width at 50 and 150 °C between the two samples can be attributed to greater restriction on the rotational and translational motion of the phosphate groups in the 2OH-PBI membranes. An additional ^{31}P line-width contribution from structural heterogeneity in the 2OH samples is inferred, as discussed in more detail later.

The ^{1}H spectra at 50 and 150 °C for both the 2OH-PBI and para-PBI samples are shown in the Figures 4 and 5, respectively. At both 50 and 150 °C both samples displayed a main asymmetric peak centered at 6 ppm and a small peak close to 0 ppm. At 50 °C the line width of the main asymmetric peak was

dx.doi.org/10.1021/jp304761t | J. Phys. Chem. B 2012, 116, 12545−12551

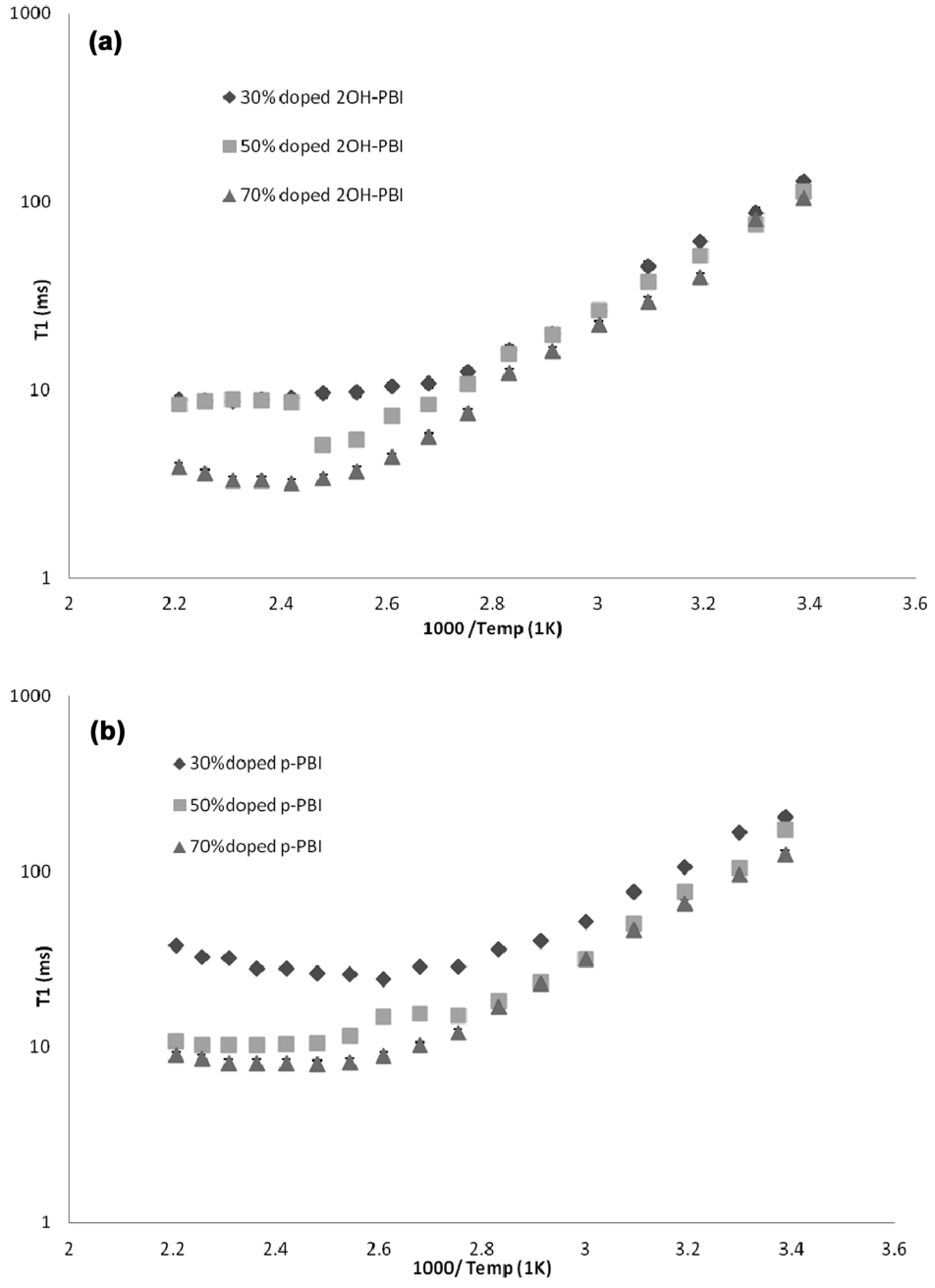

Figure 7. Arrhenius plots of ^{31}P T_1 data for (a) 2OH-PBI and (b) para-PBI (−2 ppm peak) with 30, 50, and 70% phosphoric acid concentration.

observed to increase with increased acid concentration for the 2OH-PBI sample. However, the para-PBI sample showed a decrease in line width with increasing PA content in going from 30 to 50%, followed by a modest increase at 70%. The effect increasing PA concentration on the line width is markedly different for para PBI and 2OH PBI. A reasonable expectation of narrower lines for higher acid content membranes, based on the presence of more "free" high mobility acid, is not realized, especially in the 2OH PBI. The large increase in line width in the 70% PA 2OH PBI sample is attributed to heterogeneity of proton environments through strong interaction between the acid and the polymer. The effect of elevated temperature on the spectra is to produce a modest motional line narrowing, as will be discussed momentarily.

Figure 6 shows ^1H line widths for both 2OH-PBI and para-PBI samples as a function of temperature. The general trend in the line width was a decrease with increasing temperature for both samples. A decrease in line width is usually an indication of increased mobility. A comparison of the two samples at equivalent PA content shows the 2OH-PBI sample having the smaller line width at 30% acid content. However, at both 50 and 70% PA content, the para-PBI line width is narrower. This would indicate that, at 50 and 70% PA content, the cation groups are less restricted in the para-PBI samples compared to those in the 2OH-PBI samples. As mentioned above, an alternative and more likely additional factor in the greater broadening of the ^1H NMR spectra in the 2-OH samples at higher acid content is larger site heterogeneity. The line width of the 30% PA para-PBI sample exhibits only a very modest temperature dependence, suggesting correspondingly weaker line-broadening interactions between the PA and host PBI compared to the other samples.

dx.doi.org/10.1021/jp304761t | J. Phys. Chem. B 2012, 116, 12545−12551

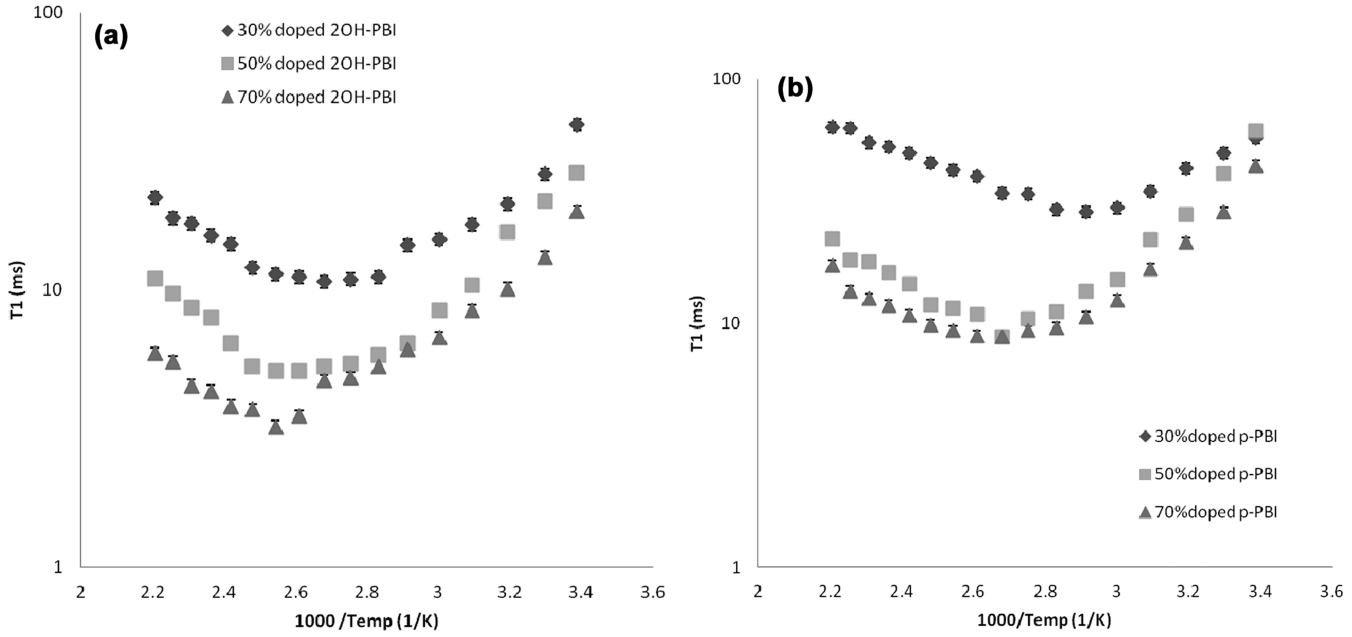

Figure 8. Arrhenius plots of ^{1}H T_1 data for (a) 2OH-PBI and (b) para-PBI with 30, 50, and 70% phosphoric acid concentration.

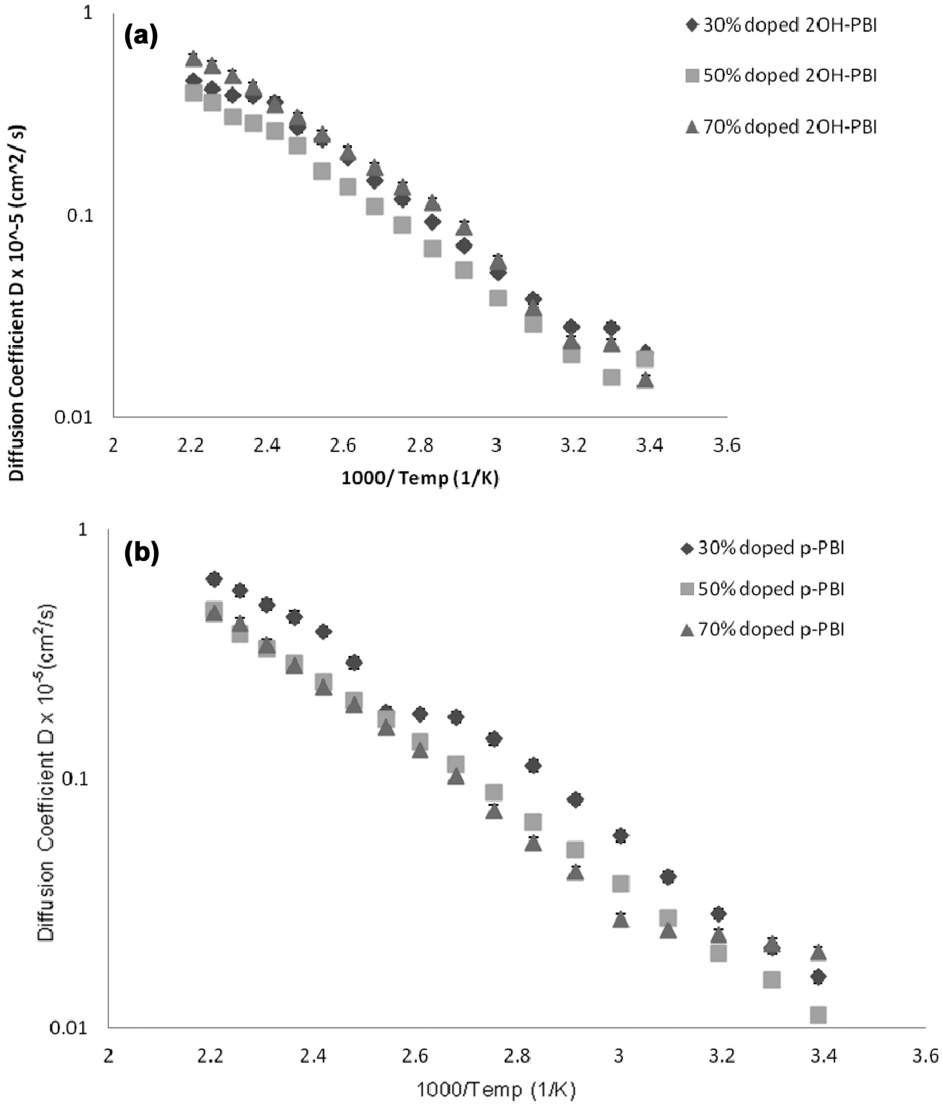

Figure 9. ^{1}H self-diffusion data for (a) 2OH-PBI and (b) para-PBI with 30, 50, and 70% phosphoric acid concentration as function of inverse temperature.

dx.doi.org/10.1021/jp304761t | J. Phys. Chem. B 2012, 116, 12545−12551

2. ^{1}H and ^{31}P T_1 data. Arrhenius plots of ^{31}P and ^{1}H T_1 data are shown in Figures 7 (for the ∼0−2 ppm phosphorus peak) and 8, respectively, for both the 2OH-PBI and para-PBI samples. The general trend was a decrease to a broad minimum or plateau with increasing temperature. For the ^{31}P nuclei the T_1 minimum occurs within the range of 383−443 K, while for the ^{1}H nuclei, it occurs between 333 and 393 K. Although it is possible that the difference observed in the location of the T_1 minimum for a given sample could be due to the difference in frequencies, it seems more likely to suggest a lack of correlation between the phosphorus and proton species. For spin 1/2 nuclei the most dominant T_1 relaxation mechanism is dipole−dipole, which is a short-range interaction. Additionally, at fixed PA content, the 2OH-PBI sample has shorter T_1. In general, shorter T_1s are usually associated with more restriction, or a greater relaxation strength "prefactor", which in the present context refers to strong interaction between the PA and PBI.[16] Again, the results for the 30% para-PBI are noteworthy in that they show the highest T_1 values and lowest temperature T_1 minimum for both nuclei. In our interpretation, this provides additional evidence for weaker interaction between PA and PBI for this sample, as alluded to previously in the context of the discussion for Figure 6. This supports the ^{31}P spectra data which shows greater line width for the 2OH-PBI samples.

Additionally, it was also observed that increasing the acid content from 30 and 50 wt % resulted in an increase in the temperature at which the ^{1}H T_1 minimum or plateau occurred for both samples, but that further increase caused no change.

3. ^{1}H Self-Diffusion Coefficients *D*. ^{1}H *D* data as a function of temperature for the 2OH-PBI and para-PBI samples are presented in the Figure 9. Due to the very short spin−spin relaxation times, measurements of ^{31}P *D*'s were not possible under the current spectrometer capabilities. The general trend is an increase in *D* with increasing temperature. For the para-PBI sample the 30% PA content sample gave the highest *D* values over almost the entire temperature range, with the 50 and 70 wt % samples giving almost identical results with increasing temperature.

Activation energies calculated from the ^{1}H *D* values are given in Table 1. While these values are consistent with that of a proton-hopping mechanism,[17] they increase with increasing acid content and approach the literature value of 0.32 eV for 100% phosphoric acid.[18]

Table 1. Calculated Activation Energies from the ^{1}H Self-Diffusion Coefficient Data for 2OH-PBI and para-PBI Samples As a Function of PA Content

wt % H_3PO_4	2OH-PBI (eV)	para-PBI (eV)
30	0.25	0.27
50	0.26	0.27
70	0.30	0.29

4. Discussion and Conclusions. Both 2OH-PBI and para-PBI membranes show the presence of orthophosphoric and pyrophosphoric acid groups. The 50 and 70 wt % samples especially had a third component (inferred or observed) at ∼−24 ppm which is attributed to tripolyphosphoric or higher oligomers acid. Exchange effects are observed via ^{31}P line broadening and play a significant role in the short-range transport of the phosphate nuclei albeit not leading to measurable long-range phosphate transport, as well as aiding in the long-range proton mobility. The short- and long-range dynamics in the 2OH-PBI samples were more restricted, resulting in reduced translational proton transport which was further reduced by increasing the PA content. This could be due to the presence of the OH groups, which can effectively increase the polymer's electron affinity. This, coupled with the polar nature of OH groups, would result in increased electrostatic interactions between the PA molecules and host polymer. Similar bondings have been observed in PPA mixed with phenol.[19] In that study, ^{31}P NMR spectrum of PPA showed peaks at ∼0, −14, −30, and −46 ppm attributed to H_3PO_4, chain-end phosphorus, midchain phosphorus (in tripolyphosphoric and higher oligomers), and branched phosphorus groups, respectively. However, when PPA was mixed with phenol, the spectrum at 100 °C showed additional peaks at ∼−5 and −20 ppm, attributed to $PhOP(O)(OH)_2$ and $PhOP(O)(OH)[OP(O)(OH)]_nOH$ groups, respectively. The peak attributed to the midchain phosphorus groups was also shifted upfield (from ∼−30 to −24 ppm) indicating less shielding. The interactions between the 2OH-PBI polymer and PPA could produce structures such as shown in Figure 10. If this is the case, it is likely that the intermolecular distance between neighboring oxygen atoms of the proton donor and acceptor groups are shorter due to increased electrostatic interactions. This would create stronger hydrogen bonds, which are a prerequisite for efficient proton transport by structural diffusion,[20] and explains the difference in ionic conductivity data obtained which show the 2OH-PBI samples having higher values compared to the para-PBI.[21] Additionally, the phenyl phosphate structure formed in this reaction creates a phosphate acid which is a stronger acid (pK_a = 1.2) than phosphoric acid (pK_a = 2.1).

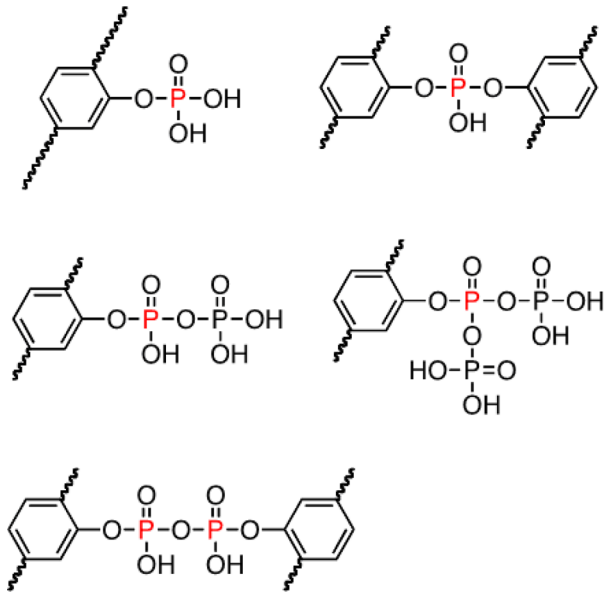

Figure 10. Various phosphorus bonding environments formed in the reaction products from the condensation of 2OH-PBI and phosphoric acid.

The effect of increasing the acid content for the para-PBI sample is a decrease in *D*. This could be due to (1) the presence of the trypolyphosphate groups, including polyphosphoric acid (PPA), which was used in the membrane preparation process, and effectively reduces the proton mass transport due to increase hydrogen bonding and possible complexation; and (2) increased electrostatic interactions between the protons and the phosphate groups in the PA molecules as well as between the PA molecule and the PBI matrix. However, it appears that, if there are indeed

dx.doi.org/10.1021/jp304761t | J. Phys. Chem. B 2012, 116, 12545−12551

complexations formed involving phosphorus linkages, their contribution to the overall proton transport may be less compared to that from the structural diffusion though increased hydrogen bonding. Activation energies obtained from the ^{1}H D data support a proton-hopping or structural diffusion mechanism, with possible assistance from fast phosphorus nuclei exchange between the various phosphate groups. However, with increasing acid content the value approaches that observed in 100% PA—a system with significant hydrogen bonding and one whose ionic conductivity is due almost entirely to proton transport.[18]

AUTHOR INFORMATION

Corresponding Author

*E-mail: snsuarez@brooklyn.cuny.edu.

Notes

The authors declare no competing financial interest.

REFERENCES

(1) Li, Q.; He, R.; Jensen, J. O.; Savinell, R.; Bjerrum, N. *Prog. Polym. Sci.* **2009**, *34*, 449−477.
(2) Li, Q.; He, R.; Jensen, J. O.; Bjerrum, N. *Chem. Mater.* **2003**, *15*, 4896−4915.
(3) Santiago, E. I.; Isidoro, R. A.; Dresch, M. A.; Matos, B. R.; Linardi, M.; Fonseca, F. C. *Electrochim. Acta* **2009**, *54*, 4111−4117.
(4) Chung, T. S. *J. Macromol. Sci.* **1997**, *C37*, 277−301.
(5) Bouchet, R.; Siebert, E. *Solid State Ionics* **1999**, *118*, 287−299.
(6) Fontanella, J. J.; Wintersgill, M. C.; Wainright, J. S.; Savinell, R. F.; Litt, M. *Electrochim. Acta* **1998**, *43*, 1289−1294.
(7) Kongstein, D. E.; Berning, T.; Borresen, B.; Seland, F.; Tunold, R. *Energy* **2007**, *32*, 418−422.
(8) Xing, B.; Savadogo, O. *J. New Mater. Electrochem. Systems* **1999**, *2*, 95−101.
(9) Lassegues, J. C. Mixed Inorganic-Organic systems: the acid/polymer blends. In *Proton Conductors, Solids, Membranes and Gels-Materials and Devices*; Colomban, Ph., Ed.; Cambridge University Press: Cambridge, UK, 1992; p 311.
(10) Xiao, L.; Zhang, H.; Scanlon, E.; Ramanathan, L. S.; Chloe, E.-W.; Rogers, D.; Apple, T.; Benicewicz, B. C. *Chem. Mater.* **2005**, *17*, 5328−5333.
(11) Xiao, L.; Zhang, H.; Jana, T.; Scanlon, E.; Chen, R.; Chloe, E.-W.; Ramanathan, L. S.; Benicewicz, B. C. *Fuel Cells* **2005**, *5*, 287−295.
(12) Jayakody, J. R. P.; Chung, S. H.; Durantino, L.; Zhang, H.; Xiao, L.; Benicewicz, B. C.; Greenbaum, S. G. *J. Electrochem. Soc.* **2007**, *154*, B242−B246.
(13) Stejskal, E. O.; Tanner, J. E. *J. Chem. Phys.* **1965**, *42*, 288−292.
(14) Fukushima, E.; Roeder, S. B. *Experimental Pulse NMR: A Nuts and Bolts Approach*; Addison-Wesley Longman: Reading, MA, 1981.
(15) Crutchfield, M. M.; Callis, C. F.; Irani, R. R.; Roth, G. C. *Inorg. Chem.* **1962**, *1*, 813−817.
(16) Bloembergen, N.; Purcell, E. M.; Pound, R. V. *Phys. Rev.* **1948**, *73*, 679−712.
(17) Chandra, S. *Proceedings of the II International Symposium on Solid State Devices*; Chowdari, B. V., Radakrishna, S., Eds.; World Scientific Publication: Singapore, 1988.
(18) Dippel, T.; Kreuer, K. D.; Lassegues, J. C.; Rodriguez, D. *Solid State Ionics* **1993**, *61*, 41−46.
(19) So, Y.-H.; Heeschen, J. *J. Org. Chem.* **1997**, *62*, 3552−3561.
(20) Vilciauskas, L.; Tuckerman, M.; Bester, G.; Paddison, S.; Kreuer, K.-D. *Nat. Chem.* **2012**, *4*, 461−466.
(21) Yu, S.; Benicewicz, B. C. *Macromolecules* **2009**, *42*, 8640−8648.